

Role of ELP6 in tumour progression and impact on ERK1/2 signalling pathway inhibitors in skin cutaneous melanoma

YING LIU^{1*}, QINRONG WANG^{1*}, QIAN LI² and PENG REN³

¹Key Laboratory of Endemic and Ethnic Diseases, Ministry of Education and Key Laboratory of Medical Molecular Biology of Guizhou Province, Guizhou Medical University, Guiyang, Guizhou 550004, P.R. China; ²Department of Pharmacy, Guizhou Medical University, Guiyang, Guizhou 550004, P.R. China; ³Department of Urology, The Second Affiliated Hospital of Guizhou Medical University, Kaili, Guizhou 556000, P.R. China

Received July 31, 2024; Accepted March 5, 2025

DOI: 10.3892/ol.2025.14996

Abstract. Elongator acetyltransferase complex subunit 6 (ELP6), a subunit of the elongator complex, can increase the migratory potential of melanoma cells *in vitro*. However, the clinical relevance of *ELP6* in patients with melanoma remains unclear. The present study aimed to investigate the role of *ELP6* expression in melanoma progression and association with patient survival rates. Transcriptomic data from patients with melanoma available in The Cancer Genome Atlas, Gene Expression Profiling Interactive Analysis and cBioPortal databases were analysed to evaluate the associations between *ELP6* expression levels and patient survival. *In vitro* experiments were conducted using short hairpin RNAs to downregulate *ELP6*, with a focus on cell viability, cell cycle regulation and the ERK1/2 signalling pathway. *ELP6* expression levels were significantly elevated in patients with melanoma and were associated with poor survival outcomes. Knockdown of *ELP6* resulted in decreased expression levels of p42 MAPK, reduced cell viability, G₁ phase cell cycle arrest and led to reduced responsiveness to the MEK1/2 inhibitor U0126. *ELP6* promotes melanoma progression via the ERK1/2 signalling pathway. Therefore, assessing *ELP6* expression may offer potential therapeutic strategies for patients with melanoma.

Introduction

In previous years, despite advancements in preventative measures and lifestyle changes, the incidence of skin cutaneous melanoma (SKCM) has slowed its upward trend (1,2).

However, studies demonstrate that in the United States, ~97,610 new melanoma cases were estimated to be diagnosed in 2023 (3), with cutaneous melanoma accounting for 72% of all skin cancer-related deaths (excluding basal cell carcinoma and squamous cell carcinoma) (4). These data underscore the impact of melanoma within the spectrum of skin cancer types. Consequently, there remains a pressing need for continued research efforts to explore effective treatment strategies and therapeutic targets for cutaneous melanoma.

In general, the incidence of melanoma is often associated with prolonged exposure to ultraviolet (UV) radiation, primarily from UVA and UVB spectra. Genomic analyses across various types of cancer have shown that cutaneous melanomas carry an exceptionally high mutational burden, often >10 mutations per megabase. These mutations frequently exhibit UV-specific signatures, with a notable prevalence of C-to-T transitions and G-to-T transversions (5,6). While the effects of radiation from different UV spectra can overlap owing to their ability to induce DNA mutation, UVA and UVB irradiation have distinct mechanisms in promoting melanoma. For example, UVB mainly causes damage by being absorbed by cellular components such as DNA, aromatic amino acids and unsaturated lipids, while also generating some reactive oxygen species (ROS). By contrast, UVA primarily causes damage through the production of ROS, with less direct absorption by cellular components such as DNA (7).

In contemporary melanoma management, therapeutic decision-making is fundamentally driven by comprehensive tumour genetic profiling, enabling precise alignment of targeted interventions with specific driver mutations (8,9). This approach is clearly demonstrated by BRAF inhibitors, with vemurafenib emerging as a prototypical agent demonstrating >50% objective response rates and clinically meaningful survival improvements in phase 1/2 trials involving patients with BRAF V600E mutations (10). The successful advancement of RAF-MEK inhibitors into multi-phase clinical trials (I-III) is fundamentally rooted in precision therapeutic paradigms that strategically align tumour genotype with selective pathway blockade, driving measurable survival benefits in genetically defined patient populations (11). However, this approach has its limitations. For example, some patients may exhibit a suboptimal response to these inhibitors or experience

Correspondence to: Dr Peng Ren, Department of Urology, The Second Affiliated Hospital of Guizhou Medical University, 3 Kangfu Road, Kaili, Guizhou 556000, P.R. China
E-mail: 2054568547@qq.com

*Contributed equally

Key words: elongator acetyltransferase complex subunit 6, p42 MAPK, melanoma

individual adverse reactions such as arthralgia, rash, nausea, photosensitivity, fatigue, cutaneous squamous-cell carcinoma, pruritus and palmar-plantar dysesthesia (12). When addressing the challenge of mitigating the aforementioned side effects, a promising approach lies in identifying an additional target for concurrent melanoma treatment, thereby enabling RAF-MEK inhibitor dose reduction while optimizing efficacy. Hence, a comprehensive exploration of the interplay between genes and melanoma development is key for devising personalized targeted treatments.

Elongator acetyltransferase complex subunit 6 (*ELP6*) (13) serves a pivotal role within the elongator complex, together with *ELP1*, *ELP2*, *ELP3*, *ELP4* and *ELP5* (14). Studies in this domain suggest that within eukaryotic cells, the *ELP6* subunit facilitates protein translation by modifying tRNAs corresponding to specific codons, including those containing the amino acids AAA (15), CAA (16) and GAA (17). Previous research has demonstrated notable associations between the *ELP* subunits and tumorigenesis, progression and/or metastasis across a spectrum of malignancies, including gallbladder carcinoma (18,19), sonic hedgehog pathway-associated medulloblastoma (20), brain cancer (21), breast carcinoma (22) and lung carcinoma (23). Notably, a previous study by Close *et al.* (24), which utilized melanoma-derived cells *in vitro*, preliminarily established a positive correlation between *ELP6* expression and the ability of melanoma to form clones and migrate. These findings suggest a potential role for inhibiting *ELP6* expression in melanoma therapy. However, there are currently no reports on whether the expression of *ELP* subunits, particularly *ELP6*, changes in patients with melanoma, whether *ELP6* gene expression levels are associated with patient survival rates and the underlying reasons for any alterations in *ELP6* expression.

Therefore, the present study aimed to systematically characterize the expression patterns and mutational profiles of *ELP1-6* in melanoma by integrating GEPIA and TCGA databases, evaluate the clinical relevance of *ELP1-6* expression levels with patient prognosis and investigate the biological function of *ELP6* in melanoma progression as well as its regulatory effects on targeted therapy sensitivity.

Materials and methods

Public data collection. Analyses were performed using the standardized pipeline of the Gene Expression Profiling Interactive Analysis (GEPIA, <http://gepia.cancer-pku.cn/index.html>) platform (25), which provides pre-integrated transcriptomic datasets from The Cancer Genome Atlas (TCGA, <https://portal.gdc.cancer.gov/>) and Genotype-Tissue Expression (GTEx, <https://gtexportal.org/home/>). Users input target gene symbols (*ELP1-6*) to activate the platform's automated analytical pipeline, which directly generates comparative expression boxplots between SKCM and normal tissues. No local data download or computational processing was performed, as all outputs were produced through the platform's self-contained analytical modules. Survival analyses utilized TCGA-derived clinical follow-up data, with patient grouped by median *ELP1-6* expression levels and Kaplan-Meier curve. Publicly available RNA-seq data of cutaneous melanoma (accession no, GSE15605) were retrieved

from the Gene Expression Omnibus (GEO, <https://www.ncbi.nlm.nih.gov/geo/>).

To examine *ELP1-6* alterations, including missense mutations, splice mutations, truncating mutations, structural variants, amplifications and deep deletions, the TCGA-SKCM dataset (PanCancer Atlas) using cBioPortal for Cancer Genomics (<https://www.cbioportal.org/>, version 3.7.29) was analysed.

Survival analysis. Essential clinical data for patients with SKCM, such as age, sex, survival time, survival status and stage, from the TCGA database were obtained. These data were then matched with whole-transcriptome profiling data for the *ELP6*^{high} (n=234) and *ELP6*^{low} (n=234) groups, categorized on the basis of the median expression of *ELP6* [median log₂(TPM + 1)=4.9055], using sample IDs. Patients without complete clinical follow-up information were excluded. Kaplan-Meier survival analysis was performed via R statistical software (version 4.1.2; <https://www.r-project.org/>; Posit Software, PBC) and the 'survival' (version 3.3.1) and 'survminer' (version 0.4.9) packages to assess the relationship between *ELP6* mRNA expression levels and survival outcomes of patients with SKCM. To compare the survival distributions between the high and low expression groups, the log rank test was applied, a non-parametric method that evaluates the observed vs. expected events (such as deaths) at each time point. The test calculates a χ^2 statistic, with the resulting P-value determining the statistical significance. P<0.05 was considered to indicate a statistically significant difference.

Chemotherapeutic sensitivity prediction. To predict drug sensitivity, the Cancer Cell Line Encyclopaedia (version no. CCLE2012, <https://sites.broadinstitute.org/ccle/>) (26) and the R package 'pRRopheticPredict' (version 0.5) that employ the ridge regression model were utilized, as previously published (27). Statistical analysis was conducted using the Wilcoxon test. P<0.05 was considered to indicate a statistically significant difference.

Cell culture. The 293T, SK-MEL-2 and A375 cell lines were obtained from Procell Life Science & Technology Co., Ltd., and were authenticated using STR analysis. A375 cells, a melanoma cell line, harbour the BRAF V600E mutation (28), and SK-MEL-2 cells, also melanoma-derived, harbour an N-RAS mutation (29), both of which are relevant to the study of melanoma. The cell lines were cultured according to standard protocols in medium supplemented with 10% foetal bovine serum (FBS) and 100 µg/ml penicillin. The cells were maintained at 37°C in a humidified atmosphere with 5% CO₂.

Cell counting kit-8 (CCK-8) cytotoxicity assay. The target cells were seeded at a density of 5,000 cells per well in 96-well plates and allowed to adhere overnight under standard culture conditions (37°C, 5% CO₂). Cells were then treated with U0126 (0, 0.1, 0.2, 0.5 or 1 µM in 0.1% DMSO) for 24 or 48 h at 37°C. Following treatment, the medium was replaced with fresh serum-free medium supplemented with 10 µl of CCK-8 solution (cat. no. HY-K0301; MedChemExpress) for 1 h at 37°C. The optical density of each well was then measured at 450 nm using a microplate reader (ELx800; BioTek; Agilent

Technologies, Inc.). Background absorbance, determined from wells containing only culture medium and CCK-8 solution, was subtracted from the obtained values. Relative cell viability was calculated by comparing the absorbance of treated cells to that of untreated control cells.

RNA extraction and real-time quantitative PCR (RT-qPCR). Total RNA extraction was carried out using TRIzol reagent (Invitrogen; Thermo Fisher Scientific, Inc.) following the manufacturer's protocol. Following extraction, RNA quality and quantity were assessed using a NanoDrop spectrophotometer (Nanodrop™ lite; Thermo Fisher Scientific, Inc.) or agarose gel electrophoresis. cDNA synthesis was subsequently performed using reverse transcriptase M-MLV (RNase H-), and RT-qPCR was subsequently conducted using TB Green® Premix Ex Taq™ II (Tli RNaseH Plus; Takara Bio, Inc.) on a real-time PCR System (Bio-Rad Laboratories, Inc.) under the following thermocycling conditions: 95°C for 30 sec; 39 cycles of 95°C for 10 sec, 56°C for 15 sec and 72°C for 15 sec. Melt curve analysis was performed at the following thermocycling conditions: 95°C for 15 sec, 55°C for 15 sec and continuous heating from 55-95°C at 0.5°C increments every 5 sec to verify amplification specificity. Gene expression levels were normalized to those of GAPDH, and relative expression was calculated using the $2^{-\Delta\Delta C_q}$ method (30,31). To ensure accuracy and reproducibility, triplicate experiments were performed for each sample. Target genes were amplified using the following primers: ELP6 forward (F), 5'-TGGCTGTGCTAGACTTCA T-3' and reverse (R), 5'-GTCATTCTCCTCATCCTCC-3'; GAPDH F, 5'-ACAACTTTGGTATCGTGGAAGG-3' and R, 5'-GCCATCACGCCACAGTTTC-3'; proliferating cell nuclear antigen (PCNA) F, 5'-CCTGCTGGGATATTAGCTCCA-3' and R, 5'-CAGCGGTAGGTGTCTGAAGC-3'; Ki67 F, 5'-ACG CCTGGTTACTATCAAAAGG-3' and R, 5'-CAGACCCAT TTACTTGTGTTGGA-3'; KARS1 F, 5'-ACAGATAATGAG CCCTTTG-3' and R, 5'-GTTGTTGGAGTCCGTGAG-3'; p44 MAPK F, 5'-CTACACGCAGTTGCAGTACAT-3' and R, 5'-CAGCAGGATCTGGATCTCCC-3'; and p42 MAPK F, 5'-CATGTCTGAAGCGCAGTAAGATT-3' and R, 5'-TAC ACCAACCTCTCGTACATCG-3'.

Western blotting. ShCtrl and shELP6-3 293T cell lines were treated with cycloheximide (CHX, cat. no. HY-12320; MedChemExpress) 0 or 10 µg/ml in serum free medium at 37°C with 5% CO₂ for 0 or 24 h, while shCtrl and shELP6 A375 cells were exposed to CHX (0 or 10 µg/ml) under the aforementioned conditions for 0, 12 or 24 h. Cellular proteins were extracted using RIPA lysis buffer (cat. no. r0010-100; Beijing Solarbio Science & Technology Co., Ltd.) supplemented with PMSF (cat. no. P0100; Beijing Solarbio Science & Technology Co., Ltd.) and protease/phosphatase inhibitor cocktail (cat. no. P6730; Beijing Solarbio Science & Technology Co., Ltd.). After lysis on ice, the lysates were centrifuged at 16,000 x g for 30 min at 4°C to collect the protein-containing supernatant, which was then quantified using the Bradford assay. Equal amounts (50 µg) of protein samples were separated using 10 or 12% SDS-PAGE gels and transferred onto polyvinylidene fluoride membranes (cat. no. SEQ00010; Merck KGaA). The membranes were blocked with 5% milk at room temperature for 1 h and incubated overnight at 4°C with primary antibodies

targeting ERK1/2 (cat. no. 51068-1-AP; 1:1,000; Proteintech Group, Inc.), phospho-ERK1/2 (cat. no. Thr202/Tyr204) (cat. no. 28733-1-AP; 1:500; Proteintech Group, Inc.) or GFP (cat. no. 66002; 1:3,000; Proteintech Group, Inc.), together with GAPDH (cat. no. 60004; 1:3,000; Proteintech Group, Inc.) or tubulin (cat. no. 66031; 1:3,000; Proteintech Group, Inc.) as the housekeeping proteins for normalization. After incubation with goat anti-mouse (cat. no. SA00001-1; 1:5,000; Proteintech Group, Inc.) or goat anti-rabbit (cat. no. SA00001-2; 1:5,000; Proteintech Group, Inc.) secondary antibodies at room temperature for 1 h, protein bands were subsequently visualized using the Immobilon Western Chemiluminescent HRP substrate (cat. no. WBKLS0100; Merck KGaA).

Plasmid constructs. The overexpression vector was constructed by amplifying *ELP6* cDNA from 293T cells using PCR. PCR amplification was performed with PrimeSTAR HS DNA polymerase (cat. no. R010A; Takara Bio, Inc.) using the following primers: F, 5'-GGAATTCATGTTTCGTGGAACCTTAATAA CC-3' and R, 5'-AAGGTACCTCACAGAACAGCAGGAGAC AT-3'. The following thermocycling conditions were used: 98°C for 2 min; 35 cycles of 98°C for 10 sec, 55°C for 15 sec, 72°C for 1 min and 72°C for 5 min. The PCR product was separated on a 1% agarose gel (cat. no. 9012-36-6, Sangon Biotech Co., Ltd.) stained with GeneRed (cat. no. RT211, Tiangen Biotech Co., Ltd.), and the target band (~0.8 kb) was excised and purified using a Gel Extraction Kit (cat. no. DP209-02; Tiangen Biotech Co., Ltd.). Both the PCR product and the PEGFP-C2 plasmid (Runyan Laboratory Reagents Co., Ltd.) were subsequently digested with *EcoRI* (cat. no. 1040S; Takara Bio, Inc.) and *KpnI* (cat. no. 1068S; Takara Bio, Inc.) enzymes. The digested fragments were ligated together via T4 DNA ligase (cat. no. 2011A; Takara Bio, Inc.) and transformed into competent *Escherichia coli* DH5α cells (cat. no. 9027; Takara Bio, Inc.). Positive transformants were selected on LB agar plates containing 50 µg/ml kanamycin (cat. no. K8020; Beijing Solarbio Science & Technology Co., Ltd.), and the resulting plasmid was purified using the Rapid Plasmid Extraction Kit (cat. no. DP105-02; Tiangen Biotech Co., Ltd.) according to the manufacturer's protocol. Verification of the construct was achieved through restriction enzyme digestion and Sanger sequencing (data not shown), which confirmed the successful integration of *ELP6* into the pEGFP-C2 plasmid. The p42-MAPK-pcDNA3.10V5-HisB plasmid was obtained from Genewiz, Inc.

Cell transfection. The 293T or A375 cells were transfected with Lipofectamine™ 2000 transfection reagent (cat. no. 11668019; Thermo Fisher Scientific, Inc.) in accordance with the manufacturer's instructions. Briefly, 293T or A375 cells were seeded to achieve 60-70% confluency prior to transfection. Plasmid DNA (2 µg/well in 6-well plates) or siRNA (50 nM final concentration) and the transfection reagent, were separately diluted in Opti-MEM reduced serum medium (cat. no. 31985070; Gibco; Thermo Fisher Scientific, Inc.), mixed at a 1:3 ratio (DNA/siRNA : reagent), and incubated at 20°C for 20 min to form complexes. These complexes were then gently added dropwise to the cells and swirled to ensure an even distribution. After incubation at 37°C (5% CO₂) for 4 h (plasmid) or 24 h (siRNA), the medium was replaced with fresh complete

Table I. shRNA sequences.

shRNA	Sequence (5'-3')
H-ELP6-psi-shRNA-1	S: GATCCGCTTTCTCTCCTTCTATCTCAATCAAGAGTTGAGATAGAAGGAGAGAA AGTTTTTTGG AS: AATTCCAAAAAACTTTCTCTCCTTCTATCTCAACTCTTGATTGAGATAGAAGG AGAGAAAGCG
H-ELP6-psi-shRNA-2	S: GATCCGGAAACTGACTCTACTCTGTGATCAAGAGTCACAGAGTAGAGTCAGT TTCTTTTTTGG AS: AATTCCAAAAAAGAACTGACTCTACTCTGTGACTCTTGATCACAGAGTAG AGTCAGTTTCCG
H-ELP6-psi-shRNA-3	S: GATCCGCAGTCATCAGAGCCATCTGATTCAAGAGATCAGATGGCTCTGATGAC TGTTTTTTGG AS: AATTCCAAAAAACAGTCATCAGAGCCATCTGATCTCTTGAATCAGATGGCTCT GATGACTGCG
Non-targeting sequence	S: GATCCGGCTTCGCGCCGTAGTCTTATCAAGAGTAAGACTACGGCGCGAAGCTT TTTTGG AS: AATTCCAAAAAAGCTTCGCGCCGTAGTCTTACTCTTGATAAGACTACGGCGC GAAGCCG

S, sense; AS, anti-sense; sh, short hairpin.

growth medium. The siRNA sequences used were as follows: siNC sense, 5'-UUCUCCGAACGUGUCACGUTT-3' and antisense, 5'-ACGUGACACGUUCGGAGAATT-3'; and lysyl tRNA synthetase (LysRS; T4) sense, 5'-GGAGAAUGUAGC AACCACUUU-3' and antisense, 5'-AGUGGUUGCUACAUCUCCUUU-3'. Cells were harvested for downstream analyses at 24, 48 72 h post-transfection.

Virus preparation. Specific short hairpin RNA (shRNA) sequences designed to target *ELP6* were integrated into psi-LVRU6GP vector backbones (GeneCopoeia, Inc.) using *Bam*HI (cat. no. 1010S; Takara Bio, Inc.) and *Eco*RI (cat. no. 1040S; Takara Bio, Inc.) restriction enzyme digestion, followed by ligation with T4 DNA ligase (cat. no. 2011A; Takara Bio, Inc.). The integrity of the construct was confirmed by Sanger sequencing (data not shown). Subsequently, viruses were generated using 293T cells. Initially, 293T cells were cultured and expanded in 10-cm dishes to an appropriate density. The constructed shRNA vector was transfected, along with the helper virus packaging vectors pMD2.G and psPAX2 (Runyan Laboratory Reagents Co., Ltd.), into 293T cells using Lipofectamine™ 2000 transfection reagent (cat. no. 11668019; Thermo Fisher Scientific, Inc.). The transfected cells were incubated at 37°C for 48 h to facilitate virus production, after which the culture supernatant was collected. Finally, the virus was stored at -80°C for subsequent experiments. The shRNA sequences used are listed in Table I.

Establishing stable cell lines via lentiviral infection. Following the transfection of 293T and A375 cells with a lentivirus targeting *ELP6*, the cells were allowed to incubate for 24 h to facilitate viral infection. The infected cells were subsequently selected using puromycin antibiotic resistance (1.5 µg/ml; cat. no. p8230; Beijing Solarbio Science & Technology Co.,

Ltd.). This selection process was maintained for 2 weeks to establish stable cell lines, including shCtrl, shELP6-2 and shELP6-3 in 293T cells, as well as shCtrl and shELP6 in A375 cells. Characterization of these cell lines, aimed at confirming the expression of the *ELP6* gene, was conducted through qPCR analysis as aforementioned.

Cell cycle analysis. shCtrl and shELP6 A375 cells (generated by lentiviral-mediated stable *ELP6* knockdown as aforementioned) were seeded into T25 flasks at a density of 1×10^6 cells per flask. After overnight culture, cells were serum-starved in serum-free medium for 24 h, followed by stimulation with complete medium containing 10% FBS for another 24 h. Cells were harvested with 0.25% trypsin (cat. no. 12604013; Gibco; Thermo Fisher Scientific, Inc.), washed twice with phosphate-buffered saline (PBS; cat. no. C10010500BT; Gibco; Thermo Fisher Scientific, Inc.), and fixed in 75% ice-cold ethanol at 4°C for 12 h. Fixed cells were washed with PBS, treated with 100 µg/ml RNase A (cat. no. 9001-99-4; Beijing Solarbio Science & Technology Co., Ltd.) at 37°C for 30 min to digest RNA and then stained with 50 µg/ml propidium iodide (PI) (cat. no. 25535-16-4; Beijing Solarbio Science & Technology Co., Ltd.) in the dark at 4°C for 30 min for DNA quantification. For flow cytometric analysis, a FACSVerse flow cytometer (BD Biosciences) equipped with PI fluorescence captured was used, and cell cycle distribution (G0/G1, S, G2/M phases) was quantified using ModFit LT software (version 4.0.5; Verity Software House, Inc.).

Statistical analysis. All experiments were independently conducted at least three times. Data were expressed as mean ± SEM. Statistical comparisons were performed using the two-tailed unpaired student's t-test for two-group analyses. For multi-group comparisons, one-way ANOVA was applied

followed by Tukey's test or Dunnett's test. Non-normally distributed data were analysed with Wilcoxon paired signed-rank test. $P < 0.05$ was considered to indicate a statistically significant difference.

Results

ELP6 is highly expressed in SKCM. Previous investigations have demonstrated the growth-promoting effects of ELP subunits in sonic hedgehog-related medulloblastoma (15), brain cancer (16), breast cancer (17) and lung cancer (18). The present study investigated the potential anticancer activities of ELP subunits in SKCM. Using the GEPIA database, systematic examination of whether the mRNA expression levels of ELP subunits (including ELP1-6) were altered in various types of cancer was conducted. Compared with that in normal tissues, the mRNA expression levels of *ELP1*, *ELP2*, *ELP3* and *ELP4* in SKCM remained unchanged (Fig. 1A-D). By contrast, when the same criteria were used, the expression levels of *ELP5* and *ELP6* SKCM were significantly increased compared with that in normal tissues (Fig. 1E and F).

Next, the potential impact of increased expression levels of ELP subunits on clinical outcomes was examined. Using transcriptomic data from the GEO database (dataset accession no. GSE15605), receiver operating characteristic curve analysis demonstrated that *ELP6* expression levels significantly distinguished SKCM samples from normal tissues, with an area under the curve of 0.794 (95% CI, 0.666-0.901) (Fig. 1G). Using the GEPIA database to generate Kaplan-Meier curves, it was determined that increased mRNA expression levels of *ELP1*, 2, 3, 4 and 5 did not have a significant effect on the prolonged time to recurrence or death (Fig. 1H-L). However, increased expression levels of the specific subunit *ELP6* were significantly associated with shorter overall survival (OS) in patients with SKCM (Fig. 1M), whereas increased *ELP6* expression levels had no significant impact on disease-free survival (Fig. S1A). The survival analysis from the GEPIA database (Fig. 1M) showed lower survival rates between 100 to 200 months, followed by a reversal of survival trends between 250 to 300 months. To account for this, transcriptome profiling data was utilized with complete clinical information from the TCGA-SKCM cohort, which includes patients with SKCM categorized into two groups based on the median expression level of *ELP6*: OS-*ELP6*^{high} (n=229) and OS-*ELP6*^{low} (n=229). To further refine the analysis, the follow-up period was restricted to the first 18 years (216 months). The truncated analysis still demonstrated significant survival differences (Fig. 1N; $P < 0.05$), with higher *ELP6* expression levels being associated with poorer prognosis and a shorter median OS in patients with SKCM. When comparing OS across different stages, *ELP6* expression levels were closely associated with poorer OS in both stage 0/I/II (Fig. S1B) and stage III/IV groups (Fig. S1C). Moreover, subgroup analysis based on sex demonstrated that elevated *ELP6* expression levels were significantly associated with worse OS specifically in male patients with SKCM (Fig. S1D and E).

To investigate the underlying causes of the abnormal expression of *ELP6*, the cBioPortal database was utilized to analyse the mutation rates of *ELP1*, *ELP2*, *ELP3*, *ELP4*, *ELP5* and *ELP6* in TCGA-SKCM (PanCancer Atlas) in 363 SKCM

samples. As shown in Fig. S2A, the incidence of mutations in *ELP1-6* was markedly low in SKCM. Notably, while the mutation rates in *ELP1*, *ELP2*, *ELP3*, *ELP4* and *ELP5* were 6.0, 2.8, 4.0, 2.2 and 2.2%, respectively, *ELP6* presented the lowest mutation rate at 1.4%, which included four missense mutations and one amplification, suggesting that there were no significant alterations in the sequence of *ELP6* that could account for its upregulation. Moreover, associations between *ELP6* expression levels and the sex or age of patients with SKCM were explored using TCGA clinical characteristics; however, no significant differences were detected either between the ≥ 50 and < 50 years of age groups, or between males and females (Fig. S2B-E).

Positive association between ELP6 expression levels and cell proliferation capability. To ascertain whether increased *ELP6* expression contributed to SKCM progression, Gene Set Enrichment Analysis (GSEA) was performed to predict potential mediators of its effects. This analysis showed that cell cycle progression pathways-driven by CDK1, *E2F1-4*, and *PCNA*-were positively enriched (data not shown), suggesting that *ELP6* may promote tumorigenesis by enhancing proliferative signalling. To further validate this association, *ELP6*-knockdown clones were generated in 293T cells using four different shRNAs: shCtrl, sh*ELP6*-1, sh*ELP6*-2 and sh*ELP6*-3. The RNA knockdown efficiency reached ~20 and 70% inhibition of *ELP6* expression levels in sh*ELP6*-2 and sh*ELP6*-3 cells, respectively (Fig. 2A), whereas no significant changes were observed in sh*ELP6*-1 (data not shown). Therefore, sh*ELP6*-2 and sh*ELP6*-3 were selected for the CCK-8 assay. *ELP6* knockdown led to a significant reduction in cell viability (Fig. 2B and C). Given the significant inhibitory effects observed with sh*ELP6*-3, sh*ELP6*-3 was used to establish stable *ELP6* knockdown clones in A375 cells and in SK-MEL-2 cells, denoted as sh*ELP6*-A375 (Fig. 2D) and sh*ELP6*-SK-MEL-2 (Fig. S3A). Consistent with these results, *ELP6* suppression led to a significant reduction in the proliferation rate, as demonstrated by the CCK-8 assay (Figs. 2E and S3B).

In response to uncontrolled proliferation conditions, cells can experience excessive activation of both Ki67 (32) and PCNA (33,34). Therefore, the mRNA expression levels of Ki67 (Fig. 2F and G) and PCNA (Fig. 2H and I) were analysed in stable cell lines with varying levels of *ELP6* expression. Downregulation of Ki67 and PCNA mRNA expression levels in the sh*ELP6*-2, sh*ELP6*-3 and sh*ELP6* cell lines were observed, compared with their respective controls. To further confirm the role of *ELP6* expression in tumour progression, a GFP-tagged *ELP6* plasmid was constructed and transiently transfected into both the sh*ELP6*-2 and sh*ELP6*-3 cell lines, in which *ELP6* was silenced as aforementioned. The reintroduction of *ELP6* resulted in a significant increase in PCNA mRNA expression levels (Fig. 2J and K; Fig. S3C), providing evidence that *ELP6*-mediated tumour promotion is linked to cell proliferation.

Next, the impact of *ELP6* on the re-entry of quiescent A375 cells into the cell cycle when stimulated with serum was assessed. After a 24 h incubation of both sh*ELP6* and shCtrl cells with FBS, flow cytometry was used to assess the cells ability to progress through the G₁ phase (Fig. 2L-N). sh*ELP6*

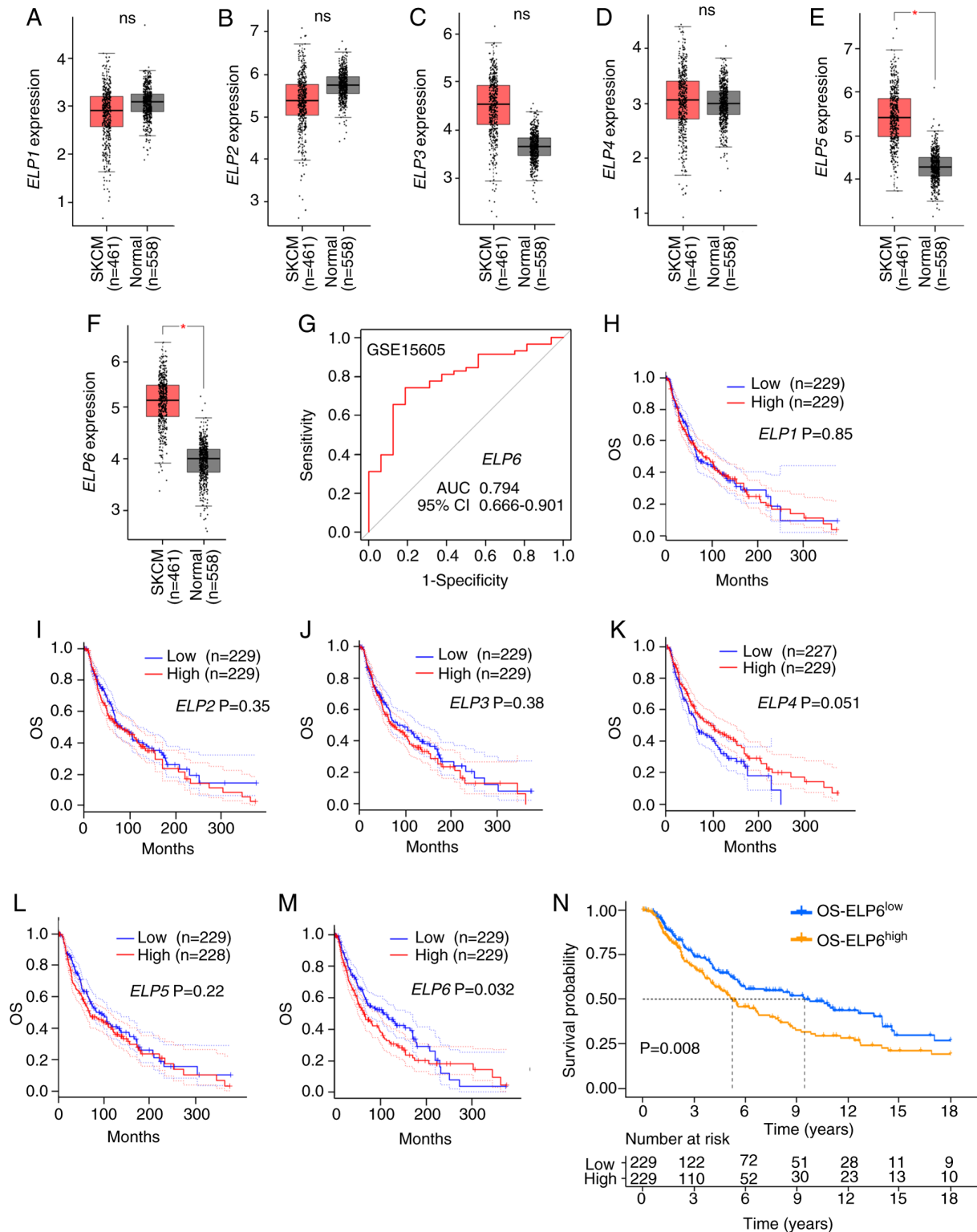


Figure 1. Prognostic impact of *ELP1*, *ELP2*, *ELP3*, *ELP4*, *ELP5* and *ELP6* expression levels in patients with SKCM. The transcriptional levels of (A) *ELP1* (ns), (B) *ELP2* (ns), (C) *ELP3* (ns), (D) *ELP4* (ns), (E) *ELP5* (*P<0.05) and (F) *ELP6* (*P<0.05) in the normal (grey) and SKCM (red) groups according to the GEPIA database. (G) The predictive performance of *ELP6* to distinguish between normal and SKCM samples was high, demonstrated using the GSE15605 dataset. (H-M) Kaplan-Meier plotter analysis of OS rates between patients with SKCM stratified into the following groups: (H) *ELP1*^{high} and *ELP1*^{low}, (I) *ELP2*^{high} and *ELP2*^{low}, (J) *ELP3*^{high} and *ELP3*^{low}, (K) *ELP4*^{high} and *ELP4*^{low}, (L) *ELP5*^{high} and *ELP5*^{low} and (M) *ELP6*^{high} and *ELP6*^{low}, according to GEPIA data. (N) The Kaplan-Meier survival curves by *ELP6* transcript levels in patients with TCGA-SKCM (n=458). *ELP6*, elongator acetyltransferase complex subunit 6; SKCM, skin cutaneous melanoma; GEPIA, Gene Expression Profiling Interactive Analysis; GSE, gene set enrichment; OS, overall survival; ns, not significant.

cells predominantly experienced a G₁ arrest, with only a limited number of cells advancing to the first S phase and reaching G₂/M phases. By contrast, the control cells exhibited a greater

propensity to enter the G₁ phase. Therefore, the absence of *ELP6* prevented FBS-stimulated cell cycle re-entry, leading to the arrest of A375 cells in the G₁ phase.

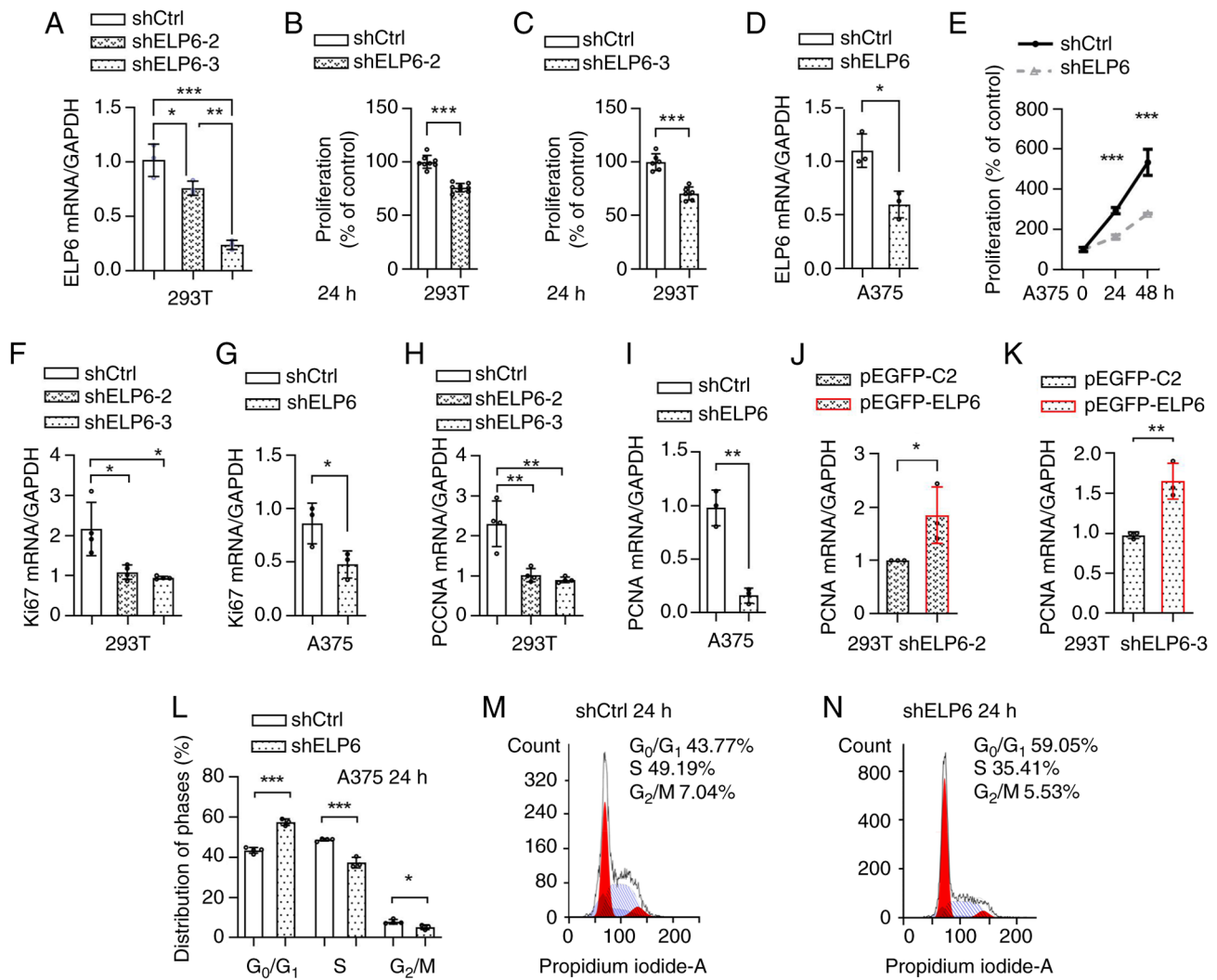


Figure 2. *ELP6* is essential for driving SKCM progression. (A) *ELP6* knockdown efficiencies were assessed in 293T cells using two independent shRNAs, shELP6-2 and shELP6-3. The viability of shCtrl, (B) shELP6-2 and (C) shELP6-3 cells was assessed at 0 and 24 h. (D) *ELP6* knockdown efficiency using shELP6 was assessed in A375 cells. (E) The viability of shCtrl and shELP6 A375 cells was assessed at 0, 24 and 48 h. The relative mRNA expression levels of Ki67 (F and G) and PCNA (H and I) were evaluated in shCtrl, shELP6-2 and shELP6-3 293T cells, as well as in shELP6 A375 cells. The levels of PCNA mRNA expression levels were evaluated in (J) shELP6-2 and (K) shELP6-3 cells after transfection with either the pEGFP-C2 or pEGFP-*ELP6* plasmid. (L) Cell cycle distribution was analysed using flow cytometry, and the percentage of cells in each phase of the cell cycle was calculated. (M) shCtrl and (N) shELP6 A375 cells were exposed to 10% serum for 24 h, followed by staining with propidium iodide. * $P < 0.05$; ** $P < 0.01$; *** $P < 0.001$. *ELP6*, elongator acetyltransferase complex subunit 6; SKCM, skin cutaneous melanoma; sh, short hairpin; m, messenger; Ctrl, control; PCNA, proliferating cell nuclear antigen.

ELP6 drives proliferation via the ERK1/2 pathway. Given the frequent activation of the RAS-BRAF-ERK1/2 pathway in melanoma and the analogous impact on the cell cycle observed with alterations in pathway activity (35), as observed with *ELP6*-mediated changes, it was investigated whether the RAS-BRAF-ERK1/2 pathway mediated *ELP6*-induced cell proliferation. In *ELP6*-deficient cells, a marked reduction in both total and phosphorylated p42 MAPK levels in 293T (Fig. 3A) and A375 (Fig. 3B) cells was observed, while total p42 MAPK levels were also significantly lower in SK-MEL-2 cells compared with that in the control cells (Fig. S3D). ERK phosphorylation efficiency (p-p42/total p42) remained unchanged in knockdown cells. However, both total and phosphorylated ERK levels (normalized to either GAPDH or tubulin) decreased correspondingly ($P < 0.01$; Fig. 3C and D), demonstrating that reduced ERK protein abundance drives the decline in active signaling molecules. qPCR analysis was

used to assess the mRNA expression levels of p42 MAPK and p44 MAPK in both the *ELP6*-normal and the *ELP6*-silenced cell lines (Fig. 3E and F). A significant decrease in the expression levels of both p42 MAPK and p44 MAPK in A375 cells following *ELP6* silencing was demonstrated (Fig. 3F). By contrast, while p44 MAPK expression levels remained stable, there was a notable increase in p42 MAPK expression levels in *ELP6*-silenced 293T cells compared with their respective parental lines (Fig. 3E).

Next, to gain insight into the influence of *ELP6* on p42 MAPK protein regulation, a GFP-tagged *ELP6* plasmid was introduced into the 293T and A375 cell lines. Transfection of the shELP6-3 293T and shELP6 A375 cells with the GFP-tagged *ELP6* plasmid resulted in a marked increase in total p42 MAPK levels, suggesting a positive relationship between *ELP6* and p42 MAPK (Fig. 3G and H). Additionally, conditions without viral infection (Fig. S4) and conditions

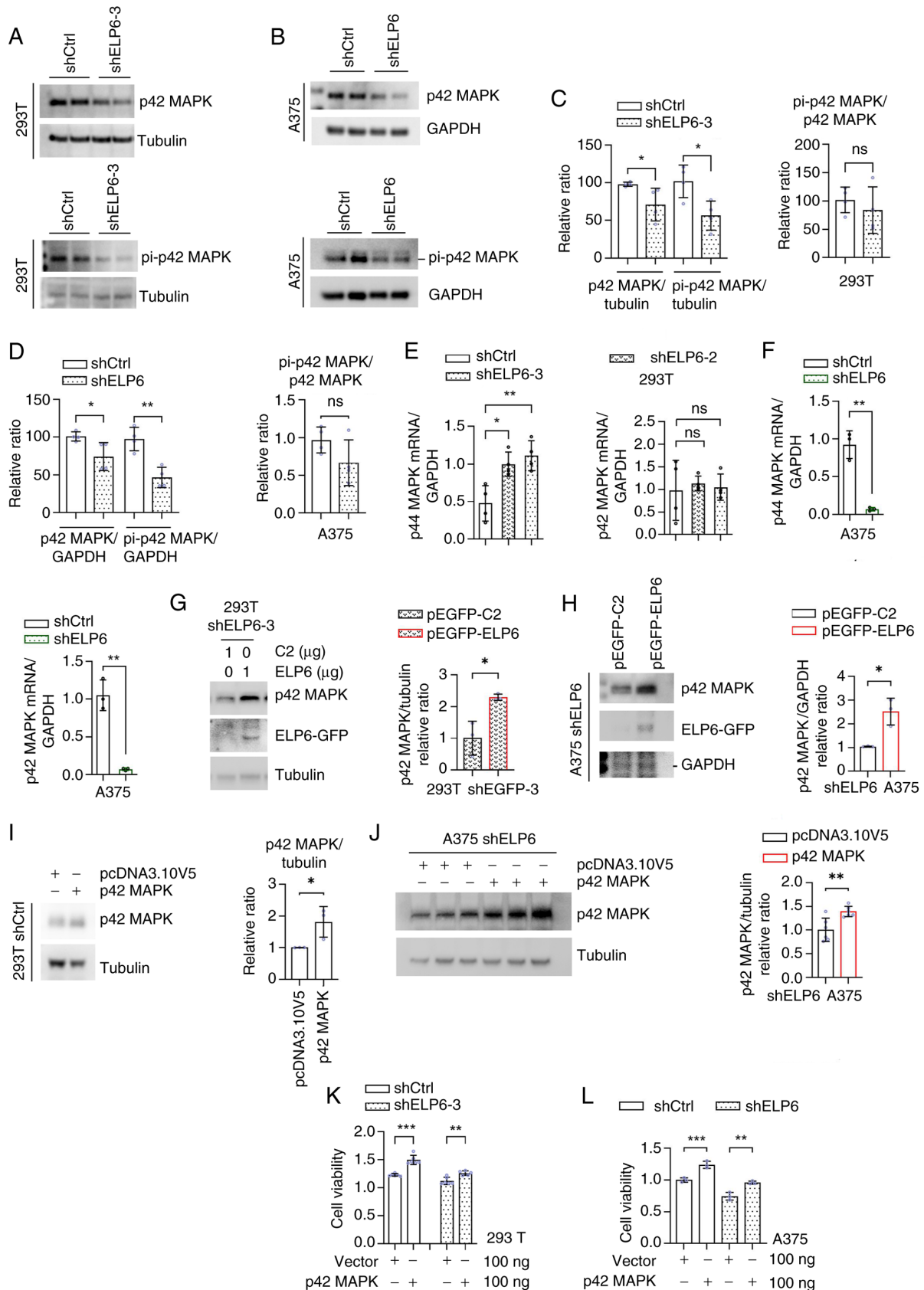


Figure 3. p42 MAPK serves a key role in mediating the proliferative effects induced by ELP6 in SKCM. Western blot analysis in shCtrl, (A) shELP6-3 293T and (B) shELP6 A375 cells of p42 MAPK or pi-p42 MAPK (Thr202/Tyr204) expression levels. (C and D) Quantification of p42 MAPK or pi-p42 MAPK (Thr202/Tyr204) protein expression levels. mRNA expression levels of p44 MAPK and p42 MAPK, normalized to the GAPDH, in the shCtrl, (E) shELP6-2, shELP6-3 293T and (F) sh-ELP6 A375 cells. Western blot analysis of ELP6-GFP, tubulin and p42 MAPK in (G) shELP6-3 293T and (H) shELP6 A375 cells transfected with either the pEGFP-C2 or pEGFP-ELP6 plasmids, with quantification of p42 MAPK protein expression levels. pcDNA3.10V5-HisB or p42 MAPK-pcDNA3.10V5-HisB transfected into shCtrl, (I) shELP6-3 293T and (J) shELP6 A375 cells were subject to western blot analysis of p42 MAPK expression levels and (K and L) cell viability assays under the same treatment conditions. * $P < 0.05$; ** $P < 0.01$; *** $P < 0.001$. ELP6, elongator acetyltransferase complex subunit 6; ns, not significant; pi, phosphorylated; SKCM, skin cutaneous melanoma; sh, short hairpin; Ctrl, control.

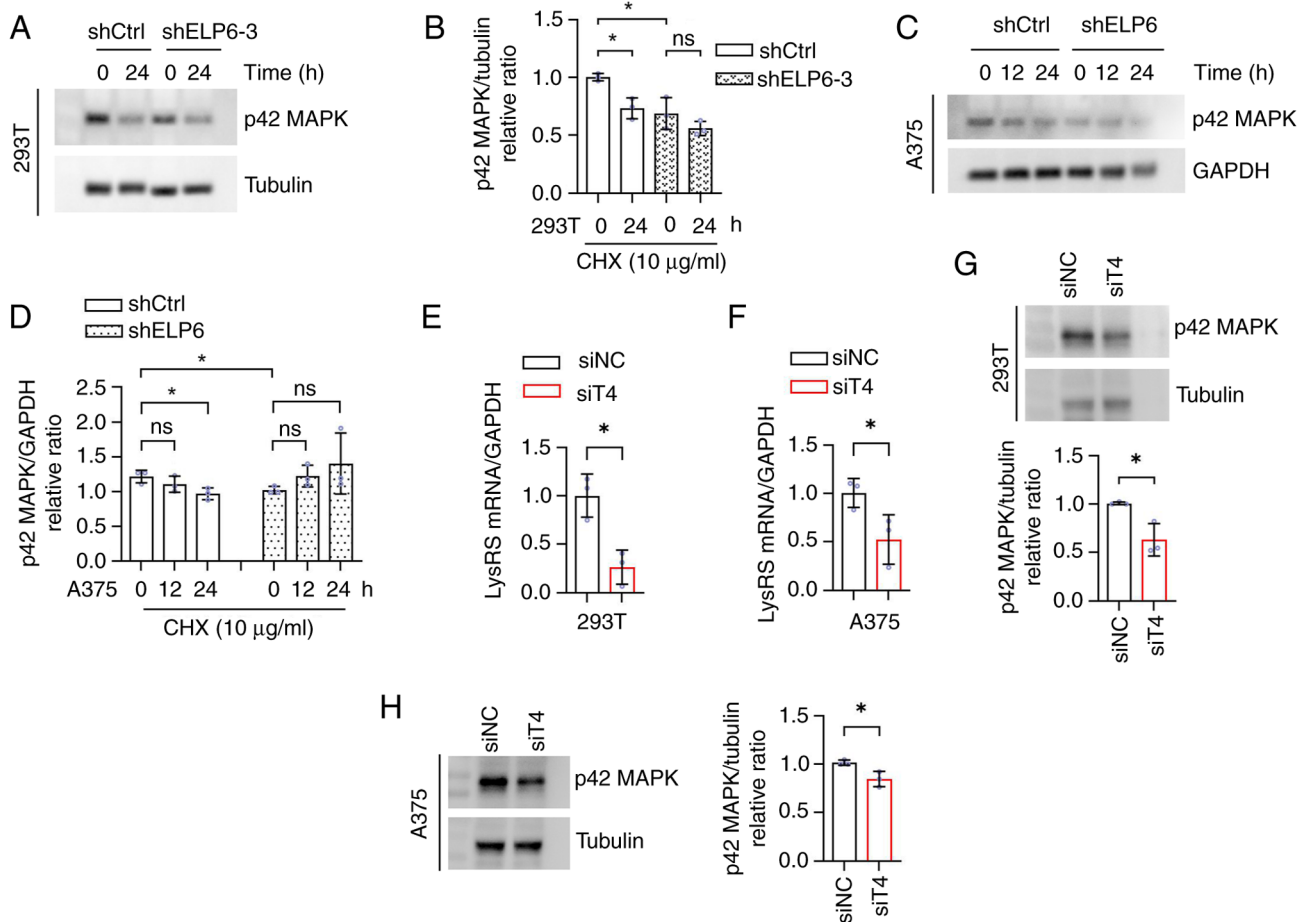


Figure 4. ELP6 stimulates p42 MAPK at the post-transcriptional level. (A) shCtrl and shELP6-3 293T cell lines were treated with CHX followed by western blotting for p42 MAPK and tubulin, quantified in (B). (C) shCtrl and shELP6 A375 cells lines were similarly treated, followed by western blotting for p42 MAPK and GAPDH, quantified in (D). The (E) 293T and (F) A375 cell lines were treated with siT4 or siNC and mRNA expression levels of LysRS, normalized to the GAPDH, were determined to detect knockdown efficiencies. p42 MAPK protein expression levels, normalized to tubulin, were determined in the (G) 293T and (H) A375 cell lines treated with siT4 or siNC. *P<0.05. ns, not significant; NC, negative control; t, transfer; sh, short hairpin; si, silencing; LysRS, lysyl tRNA synthetase; ELP6, elongator acetyltransferase complex subunit 6; SKCM, skin cutaneous melanoma; Ctrl, control; CHX, cycloheximide; siT4, LysRS siRNA.

with viral infection but without *ELP6* knockdown were examined. Transfection with pEGFP-ELP6 increased p42 MAPK protein expression regardless of viral infection or ELP6 knockdown status (data not shown). To further investigate whether *ELP6* expedited cell proliferation by increasing p42 MAPK activity, a HisB-tagged p42 MAPK plasmid was constructed and both western blot analysis and a CCK-8 assay on treated cells were conducted. A substantial increase in the intracellular p42 MAPK protein level in 293T and A375 cells upon transfection with the p42 MAPK plasmid (Fig. 3I and J). Moreover, reinstating p42 MAPK expression levels promoted proliferation in both the ELP6-disrupted cells and the control cells (Fig. 3K and L). These findings collectively underscored the pivotal contribution of p42 MAPK to ELP6-induced cell proliferation.

Given the consistent modulation of p42 MAPK protein levels and the distinct patterns of altered mRNA expression caused by changes in *ELP6* levels across both cell lines, it was hypothesized that *ELP6* may influence p42 MAPK through posttranscriptional regulation, such as by affecting the RNA translation efficiency or protein degradation rates. To investigate this, 293T and A375 cells were treated with CHX, a

eukaryotic protein synthesis inhibitor that selectively binds to ribosomes and inhibits eEF2 mediated translocation. CHX treatment resulted in a notable decrease in p42 MAPK protein levels at 16 and 24 h in shCtrl 293T and A375 cells, respectively (Fig. 4A-D). However, no significant effect was observed in cells with silenced ELP6 at 16 and 24 h, suggesting that the absence of ELP6 in cells slowed the degradation rate of the p42 MAPK protein. This finding suggested that protein degradation speed might not be the primary factor contributing to the decrease in p42 MAPK protein levels caused by ELP6 deficiency.

By modifying the wobble base, U34, of tRNA and disrupting codon-anticodon interactions, ELP6 has the potential to induce ribosomal pausing specifically at CAA and AAA codons (36), thereby impacting translation efficiency. Consequently, it was hypothesized that ELP6 could inhibit p42 MAPK protein expression by modulating codon translation rates. To investigate this possibility, qPCR was initially conducted (Fig. 4E and F), which demonstrated successful inhibition of newly synthesized LysRS, an enzyme responsible for accurately pairing lysine with the AAA codon during translation, upon silencing with siRNA, which was consistent with

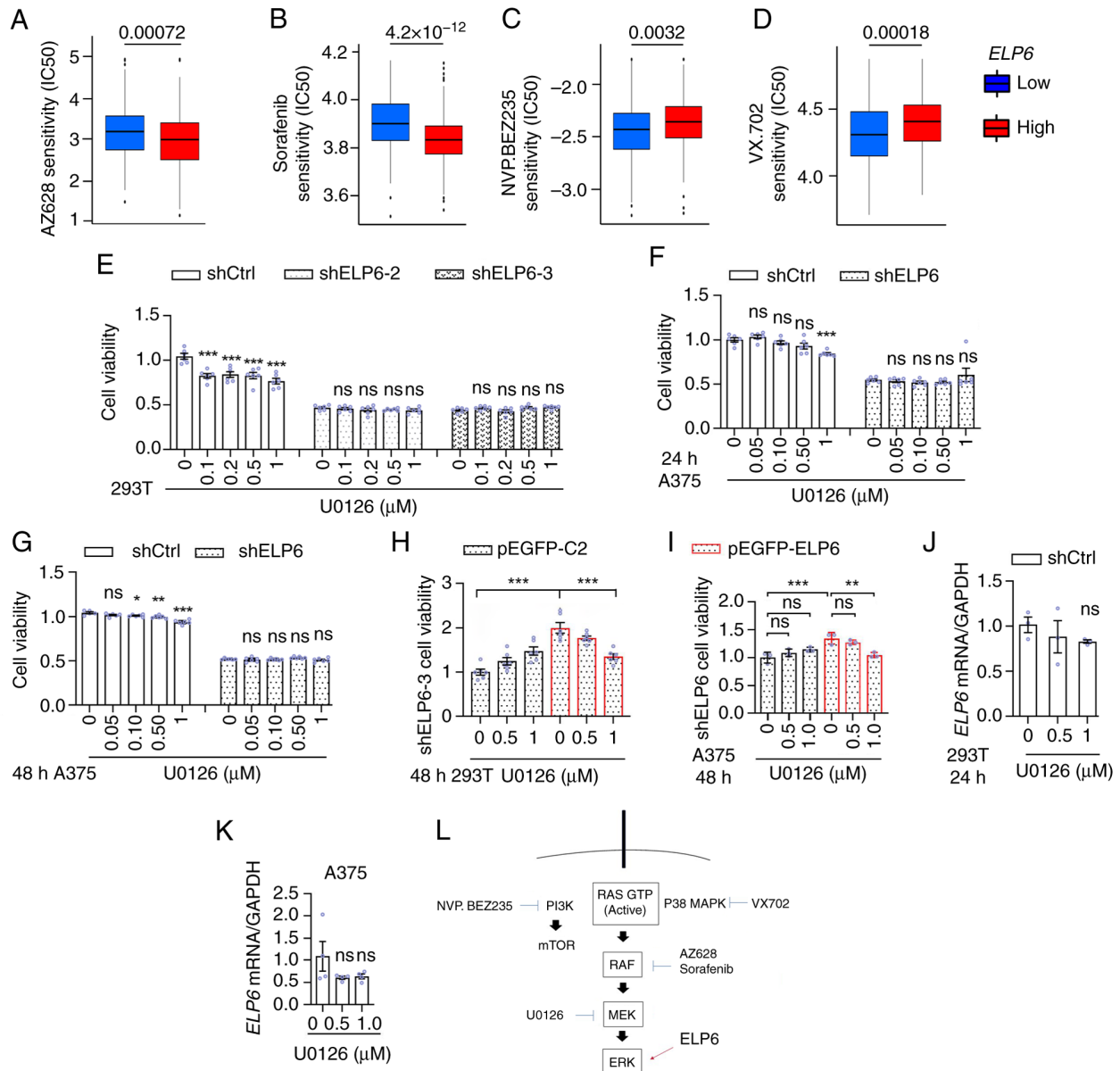


Figure 5. *ELP6* modulates drug sensitivity in melanoma cell lines. Box plots of the predicted clinical sensitivity of (A) AZ628, (B) Sorafenib, (C) NVP.BEZ235 and (D) VX702 in patients with SKCM categorized into ELP6^{high} (red) or ELP6^{low} (blue) groups from the The Cancer Atlas Genome database (n=468). (E) shCtrl, shELP6-2 and shELP6-3 293T cells were treated with U0126 for 0 and 48 h, and CCK-8 assays were performed to measure cell viability. shCtrl and shELP6 A375 cells were treated with U0126 for (F) 0, 24 and (G) 48 h, followed by a CCK-8 assay to assess cell viability. (H and I) shELP6-3 293T and shELP6 A375 cell lines were transfected with either the pEGFP-C2 or pEGFP-*ELP6* plasmid, and treated U0126 for 48 h, followed by a CCK8 assay to evaluate cell viability. shCtrl (J) -293T and (K) -A375 cells were treated with U0126 for 24 h, *ELP6* mRNA levels expression levels, normalized to GAPDH, were assessed. (L) Schematic illustrating the modulation of ERK1/2 by *ELP6*. Data are presented as mean \pm SEM. Error bars represent the SEM and each point in the graph corresponds to an individual sample. *P<0.05; **P<0.01; ***P<0.001. ns, not significant; *ELP6*, elongator acetyltransferase complex subunit 6; SKCM, skin cutaneous melanoma; Ctrl, control; CCK-8, cell counting kit-8; Sh, short hairpin; SEM, standard error of the mean.

prior findings (37). Notably, within the subgroup exhibiting decreased production of newly synthesized cellular LysRS, there was a concurrent decline in p42 MAPK protein expression (Fig. 4G and H), resembling the phenotype observed in *ELP6* deficiency. These data suggested that *ELP6* regulated p42 MAPK through ribosomal pausing.

***ELP6* sensitizes melanoma to ERK1/2 pathway inhibitors.** To investigate whether *ELP6* affected the antitumour effects of inhibitors targeting the RAF-MEK-ERK pathway, the BRAF mutation status between patients with SKCM with high and low *ELP6* expression was compared. No

significant difference in the BRAF mutation rate between the two groups was observed (Fig. S5). The R software package, pRRophetic (27), was used to predict and calculate the sensitivity values of several drugs, including the RAF inhibitors, AZ628 and sorafenib. A significant trend was demonstrated in that patients with SKCM exhibiting higher *ELP6* levels displayed greater sensitivity to AZ628 and sorafenib inhibitors compared with those with lower *ELP6* levels (Fig. 5A and B). By contrast, when the commercially available PI3K inhibitor BEZ235 and the P38 MAPK inhibitor VX702 were examined, the opposite pattern was observed (Fig. 5C and D).

Based on the aforementioned present findings which demonstrated a positive association between *ELP6* and p42 MAPK expression levels, coupled with the observation that patients lacking *ELP6* exhibit poor responses to drugs targeting the RAF-MEK-ERK pathway, a possible explanation for this sensitivity could be that patients lacking sufficient *ELP6* have less active p42 MAPK protein compared with those with higher *ELP6* expression levels. To investigate this hypothesis, shCtrl, sh*ELP6*-2 and sh*ELP6*-3 293T cells were treated with the MEK1/2 inhibitor U0126. Growth inhibition assays demonstrated that the lack of *ELP6* resulted in reduced sensitivity to U0126 (Fig. 5E). Notably, this diminished responsiveness was consistent across different cell types, as evidenced by similar trends observed in A375 cells lacking *ELP6* (Fig. 5F and G) and SK-MEL-2 cells (Fig. S6). Furthermore, reintroduction of a GFP-tagged *ELP6* plasmid restored the sensitivity of sh*ELP6*-3 and sh*ELP6* cells to U0126 (Fig. 5H and I). Short-term exposure to U0126 did not significantly affect *ELP6* mRNA levels (Fig. 5J and K), suggesting that *ELP6* functioned as an upstream regulator of ERK1/2 and was not promptly modulated by ERK1/2 activity. Taken together, these findings suggested that *ELP6* expression may have contributed, at least in part, to the diminished response of patients to RAF-MEK-ERK pathway inhibitors and highlighted its potential as a biomarker for guiding therapy.

Discussion

Melanoma presents a significant global public health challenge, contributing to 80% of skin cancer-related deaths due to its aggressive metastatic behaviour (38). Reducing melanoma mortality and improving patient responses to traditional chemotherapy remains crucial priorities in global healthcare. Previous studies have demonstrated the function of *ELP6*, a member of the elongator complex, in promoting cancer proliferation (18,19,21). For example, *ELP6* has been shown to stabilize the elongator complex, thereby enhancing the metastatic potential of melanoma (24). In the present study, bioinformatics analysis of the TCGA SKCM dataset (via the GEPIA database) demonstrated that, among the elongator complex subunits, *ELP6* was the only subunit that was both significantly upregulated in SKCM and closely associated with patient survival. However, survival analysis from the GEPIA database revealed lower survival rates between 100-200 months, followed by a reversal of survival trends between 250-300 months. The GEPIA database uses the log-rank test by default to assess survival curve differences, which assumes proportional hazard rates. When survival curves cross over, as observed between 250-300 months, this assumption is violated, which can affect the stability of the statistical results. Additionally, during the 250-300-month follow-up period, the number of patients alive in each group was relatively small (~10 individuals), which increases susceptibility to statistical fluctuations. The survival or death of a small number of individuals can disproportionately impact the survival curve. To address this issue, data were downloaded from the TCGA database for further analysis. The truncated analysis still showed significant survival differences. Based on these findings, we suggested that elevated *ELP6* expression levels may serve as a marker of SKCM

progression and has potential as a predictive biomarker for this cancer.

To further explore the underlying mechanisms, a preliminary GSEA was conducted, which demonstrated enrichment in the cell cycle signalling pathway. To investigate the potential role of *ELP6* in cell proliferation via cell cycle regulation, 293T cells, known for their high transfection efficiency (39), were used to establish effective *ELP6* knockdown during early experimental stages. *In vitro* cellular experiments demonstrated that *ELP6* downregulation significantly impaired cell proliferation, as indicated by a reduced expression of the proliferation markers Ki67 and PCNA. To establish melanoma-specific relevance despite the non-melanoma origin of 293T cells (40), these findings were validated in two melanoma cell lines: A375 (BRAF V600E mutation) (28) and SK-MEL-2 (N-RAS mutation) (29). It was demonstrated that *ELP6* knockdown consistently suppressed proliferation in both lines. Furthermore, cell cycle analysis of A375 cells further demonstrated that the loss of *ELP6* led to an increased proportion of cells in the G₁/G₀ phase. These findings suggest that *ELP6* deficiency causes cell cycle arrest in melanoma cells, hindering the transition from the G₁ to the S phase, which may contribute to tumour development and progression.

BRAF V600E mutation (41), a hallmark driver in melanoma, promotes tumorigenesis through hyperactivation of the intracellular MAPK signalling cascade, wherein p42 MAPK critically regulates the G₀/G₁ phase arrest. In the present study, it was demonstrated that *ELP6* controlled cell cycle progression at the G₁/G₀ phase and tumour proliferation, yet its potential interplay with p42 MAPK remained unexplored. Therefore, whether *ELP6* modulated both phosphorylated and total p42 MAPK protein levels was explored by using *ELP6* knockdown models in melanoma A375 cells and non-melanoma 293T cells. Notably, *ELP6* depletion led to a significant reduction in both phosphorylated and total p42 MAPK protein expression levels in both cell lines. However, the regulatory effects on p42 MAPK mRNA diverged between A375 cells (significant downregulation) and 293T cells (no significant change). This discrepancy prompted the present study to investigate whether *ELP6* modulated p42 MAPK at the post-transcriptional level. Using the protein synthesis inhibitor CHX, a time dependent decline of total p42 MAPK levels was observed in parental A375 cells, reaching statistical significance at 24 h. However, in A375 cells with low *ELP6* expression, no statistically significant difference in p42 MAPK levels was observed at 24 h. Thus, it could be considered that the downregulation of *ELP6* in melanoma cell lines led to a decrease in the p42 MAPK protein, resulting in cell cycle arrest and reduced cell proliferation, a process not driven by accelerated protein degradation. Nevertheless, it is currently unclear if *ELP6* specifically governs the translation termination fidelity of p42 MAPK, which is sensitive to translation termination control by *ELP6* during ribosomal pausing, while the translation termination of other genes such as GAPDH or tubulin are not significantly changed, which requires further investigation.

Given the high prevalence of RAF mutations in melanoma (41), significant efforts have been made to develop RAF-MEK-ERK pathway inhibitors for effective melanoma treatment (42). However, the therapeutic responses observed

in certain patients may be partially attributed to individual genetic heterogeneity. Consequently, understanding these resistance mechanisms holds promise for improving the clinical management of SKCM, especially in cases with limited therapeutic options. The results demonstrated in the present study that *ELP6* governs p42 MAPK protein may suggest that interpatient variability in *ELP6* levels could lead to differential clinical responses to MAPK cascade inhibitors, such as BRAF/MEK/ERK inhibitors. To explore this possibility, response of two sample groups (high *ELP6* levels vs. low *ELP6* levels) to inhibitors targeting the RAF-MEK-ERK signalling pathway was evaluated. This investigation indicated that patients with melanoma with lower *ELP6* levels exhibited reduced sensitivity to these inhibitors, whereas alternative pathway inhibitors, such as p38 MAPK or PI3K inhibitors, demonstrated greater efficacy. On the basis of these findings, it could be suggested that in the absence of *ELP6*, the significant reduction in the downstream key protein p42 MAPK limits the effectiveness of re-inhibiting the same pathway, such as adding RAF and MEK inhibitors, thereby failing to further restrict melanoma growth. Conversely, when *ELP6* is overexpressed or present in excess, it selectively could enhance the translation of p42 MAPK, leading to overactivation of ERK under conditions of upstream RAS and RAF mutations, supporting melanoma cell growth and survival. Therefore, in melanoma treatment, selecting appropriate therapeutic strategies based on the basis of *ELP6* expression may potentially improve patient outcomes in the future.

Melanin deposition has been recognized as having a significant effect on the efficacy of melanoma treatment. Studies have shown that, among patients undergoing radiotherapy, survival times are notably longer for amelanotic metastatic patients with melanoma than for melanotic patients. In terms of immunotherapy (43), melanin promotes melanoma progression by inhibiting immune responses through the induction of glycolysis and the activation of hypoxia-inducible factor 1 α (44,45). Additionally, melanin is associated with the production of specific neurotransmitters, such as L-DOPA (a precursor to melanin and regarded as a neurohormone) (46), which regulates the tumour microenvironment and protects cancer cells from the host immune response. In the present study, amelanotic melanoma cell lines A375 and SK-MEL-2 were used (47-50) to investigate the effects of *ELP6* on melanoma development. However, these results may not fully reflect whether the function of *ELP6* changes in the context of melanin deposition. Therefore, further evaluation using melanotic melanoma cell lines to assess the role of *ELP6* in MAPK cascade inhibitor treatment may provide a more comprehensive understanding of the role of melanin in tumour progression and treatment resistance.

In the present study, a significant increase in *ELP6* expression levels in tissue samples of patient with SKCM was demonstrated, which was significantly associated with reduced survival rates. The present findings demonstrate that *ELP6* upregulation may accelerate melanoma progression through the ERK1/2 signalling pathway. Consequently, targeting the ERK1/2 pathway potentially represents a promising therapeutic strategy for patients with elevated *ELP6* expression levels. Furthermore, the RAF-RAS-MEK pathway inhibitors,

such as ERK1/2 inhibitors, have diminished efficacy in patients with low *ELP6* expression levels, potentially due to reduced ERK1/2 activity. These insights underscore the key role of *ELP6* in both melanoma progression and treatment response, suggesting valuable implications for therapeutic intervention in the future.

Acknowledgements

Not applicable.

Funding

The present work was supported by the National Natural Science Foundation of China Grants (grant no. 81960655), Guizhou Provincial Basic Research Program [grant. no. qiankehejichu ZK(2022)372] and the Guizhou Provincial Basic Research Program [Natural Science; grant. no. ZK(2022)041].

Availability of data and materials

The data generated in the present study may be requested from the corresponding author.

Authors' contributions

YL and QW analysed data and performed experiments. QL assisted with experiments, data analysis, data verification and revision of the manuscript. PR designed the study and wrote the manuscript. YL and QL confirm the authenticity of all the raw data. All authors participated in writing the manuscript. All authors read and approved the final version of the manuscript.

Ethics approval and consent to participate

Not applicable.

Patient consent for publication

Not applicable.

Competing interests

The authors declare that they have no competing interests.

References

1. Garbe C, Keim U, Gandini S, Amaral T, Katalinic A, Holleczek B, Martus P, Flatz L, Leiter U and Whiteman D: Epidemiology of cutaneous melanoma and keratinocyte cancer in white populations 1943-2036. *Eur J Cancer* 152: 18-25, 2021.
2. Dulskas A, Cerkauskaitė D, Vincerževskienė I and Urbonas V: Trends in incidence and mortality of skin melanoma in Lithuania 1991-2015. *Int J Environ Res Public Health* 18: 4165, 2021.
3. Radomir MS, Tae-Kang K, Zorica J, Anna AB, Ewa P, Katie MD, Rebecca SM, Robert CT, Rahul S, David KC, *et al*: Malignant melanoma: An overview, new perspectives, and vitamin D signaling. *Cancers (Basel)* 16: 2262, 2024.
4. Siegel R, Miller K and Jemal A: Cancer statistics, 2017. *CA Cancer J Clin* 67: 7-30, 2017.
5. Alexandrov L, Nik-Zainal S, Wedge D, Aparicio S, Behjati S, Biankin A, Bignell G, Bolli N, Borg A, Børresen-Dale A, *et al*: Signatures of mutational processes in human cancer. *Nature* 500: 415-421, 2013.

6. Hodis E, Watson I, Kryukov G, Arolt S, Imielinski M, Theurillat J, Nickerson E, Auclair D, Li L, Place C, *et al*: A landscape of driver mutations in melanoma. *Cell* 150: 251-263, 2012.
7. Radomir MS, Jake YC, Chander R and Andrzej TS: Photo-neuro-immuno-endocrinology: How the ultraviolet radiation regulates the body, brain, and immune system. *Proc Natl Acad Sci USA* 121: e2308374121, 2024.
8. Álvarez-Prado ÁF, Maas RR, Soukup K, Klemm F, Kornete M, Krebs FS, Zoete V, Berezowska S, Brouland JP, Hottinger AF, *et al*: Immunogenomic analysis of human brain metastases reveals diverse immune landscapes across genetically distinct tumors. *Cell Rep Med* 4: 100900, 2023.
9. Hanrahan AJ and Solit DB: BRAF mutations: The discovery of Allele- and Lineage-specific differences. *Cancer Res* 82: 12-14, 2022.
10. Chapman PB, Hauschild A, Robert C, Haanen JB, Ascierto P, Larkin J, Dummer R, Garbe C, Testori A, Maio M, *et al*: Improved survival with vemurafenib in melanoma with BRAF V600E mutation. *N Engl J Med* 364: 2507-2516, 2011.
11. Schadendorf D, van Akkooi ACJ, Berking C, Griewank KG, Gutzmer R, Hauschild A, Stang A, Roesch A and Ugurel S: Melanoma. *Lancet* 392: 971-984, 2018.
12. Flaherty K, Puzanov I, Kim K, Ribas A, McArthur G, Sosman J, O'Dwyer P, Lee R, Grippo J, Nolop K and Chapman PB: Inhibition of mutated, activated BRAF in metastatic melanoma. *N Engl J Med* 363: 809-819, 2010.
13. Otero G, Fellows J, Li Y, de Bizemont T, Dirac A, Gustafsson C, Erdjument-Bromage H, Tempst P and Svejstrup J: Elongator, a multisubunit component of a novel RNA polymerase II holoenzyme for transcriptional elongation. *Mol Cell* 3: 109-118, 1999.
14. Wittschleben B, Otero G, de Bizemont T, Fellows J, Erdjument-Bromage H, Ohba R, Li Y, Allis C, Tempst P and Svejstrup J: A novel histone acetyltransferase is an integral subunit of elongating RNA polymerase II holoenzyme. *Mol Cell* 4: 123-128, 1999.
15. Winkler G, Kristjuhan A, Erdjument-Bromage H, Tempst P and Svejstrup J: Elongator is a histone H3 and H4 acetyltransferase important for normal histone acetylation levels in vivo. *Proc Natl Acad Sci USA* 99: 3517-3522, 2002.
16. Glatt S, Létoquart J, Faux C, Taylor N, Séraphin B and Müller C: The Elongator subcomplex Elp456 is a hexameric RecA-like ATPase. *Nat Struct Mol Biol* 19: 314-320, 2012.
17. Rahl P, Chen C and Collins R: Elp1p, the yeast homolog of the FD disease syndrome protein, negatively regulates exocytosis independently of transcriptional elongation. *Mol Cell* 17: 841-853, 2005.
18. Xu S, Jiang C, Lin R, Wang X, Hu X, Chen W, Chen X and Chen T: Epigenetic activation of the elongator complex sensitizes gallbladder cancer to gemcitabine therapy. *J Exp Clin Cancer Res* 40: 373, 2021.
19. Xu S, Zhan M, Jiang C, He M, Yang L, Shen H, Huang S, Huang X, Lin R, Shi Y, *et al*: Genome-wide CRISPR screen identifies ELP5 as a determinant of gemcitabine sensitivity in gallbladder cancer. *Nat Commun* 10: 5492, 2019.
20. Waszak S, Robinson G, Guden B, Smith K, Forget A, Kojic M, Garcia-Lopez J, Hadley J, Hamilton K, Indersie E, *et al*: Germline elongator mutations in sonic hedgehog medulloblastoma. *Nature* 580: 396-401, 2020.
21. Feng X, Zhang H, Meng L, Song H, Zhou Q, Qu C, Zhao P, Li Q, Zou C, Liu X and Zhang Z: Hypoxia-induced acetylation of PAK1 enhances autophagy and promotes brain tumorigenesis via phosphorylating ATG5. *Autophagy* 17: 723-742, 2021.
22. Cruz-Gordillo P, Honeywell M, Harper N, Leete T and Lee M: MCL1ELP-dependent expression of promotes resistance to EGFR inhibition in triple-negative breast cancer cells. *Sci Signal* 13: eabb9820, 2020.
23. Zhao Y, Tang D, Yang S, Liu H, Luo S, Stinchcombe T, Glass C, Su L, Shen S, Christiani DC and Wei Q: ELP2 novel variants of and in the interferon gamma signaling pathway are associated with non-small cell lung cancer survival. *Cancer Epidemiol Biomarkers Prev* 29: 1679-1688, 2020.
24. Close P, Gillard M, Ladang A, Jiang Z, Papuga J, Hawkes N, Nguyen L, Chapelle J, Bouillenne F, Svejstrup J, *et al*: DERP6 (ELP5) and C3ORF75 (ELP6) regulate tumorigenicity and migration of melanoma cells as subunits of Elongator. *J Biol Chem* 287: 32535-32545, 2012.
25. Tang Z, Li C, Kang B, Gao G, Li C and Zhang Z: GEPIA: A web server for cancer and normal gene expression profiling and interactive analyses. *Nucleic Acids Res* 45: W98-W102, 2017.
26. Barretina J, Caponigro G, Stransky N, Venkatesan K, Margolin AA, Kim S, Wilson CJ, Lehár J, Kryukov GV, Sonkin D, *et al*: The cancer cell line encyclopedia enables predictive modelling of anticancer drug sensitivity. *Nature* 483: 603-607, 2012.
27. Geeleher P, Cox N and Huang R: pRRophetic: An R package for prediction of clinical chemotherapeutic response from tumor gene expression levels. *PLoS One* 9: e107468, 2014.
28. Davide C, Paola C, Marzia C, Mirella B, Elisa S, Luca M, Jessica G, Elisabetta G, Veronica DG, Marcello M and Presta M: The Pro-oncogenic Sphingolipid-metabolizing enzyme β -galactosylceramidase modulates the proteomic landscape in BRAF(V600E)-Mutated human melanoma cells. *Int J Mol Sci* 24: 10555, 2023.
29. Whiteaker JR, Sharma K, Hoffman MA, Kuhn E, Zhao L, Cocco AR, Schoenherr RM, Kennedy JJ, Voytovich U, Lin C, *et al*: Targeted mass spectrometry-based assays enable multiplex quantification of receptor tyrosine kinase, MAP Kinase, and AKT signaling. *Cell Rep Methods* 1: 100015, 2021.
30. Livak KJ and Schmittgen TD: Analysis of relative gene expression data using Real-time quantitative PCR and the 2⁻(Delta Delta C(T)) method. *Methods* 25: 402-408, 2001.
31. Bustin SA, Benes V, Garson JA, Hellemans J, Huggett J, Kubista M, Mueller R, Nolan T, Pfaffl MW, Shipley GL, *et al*: The MIQE guidelines: Minimum information for publication of quantitative real-time PCR experiments. *Clin Chem* 55: 611-622, 2009.
32. Scholzen T and Gerdes J: The Ki-67 protein: From the known and the unknown. *J Cell Physiol* 182: 311-322, 2000.
33. Vecchiato A, Rossi CR, Montesco MC, Frizzera E, Seno A, Piccoli A, Martello T, Ninfo V and Lise M: Proliferating cell nuclear antigen (PCNA) and recurrence in patients with cutaneous melanoma. *Melanoma Res* 4: 207-211, 1994.
34. Roels S, Tilmant K and Ducatelle R: PCNA and Ki67 proliferation markers as criteria for prediction of clinical behaviour of melanocytic tumours in cats and dogs. *J Comp Pathol* 121: 13-24, 1999.
35. Hulleman E, Bijvelt JJ, Verkleij AJ, Verrips CT and Boonstra J: Nuclear translocation of mitogen-activated protein kinase p42MAPK during the ongoing cell cycle. *J Cell Physiol* 180: 325-333, 1999.
36. Nedialkova D and Leidel S: Optimization of codon translation rates via tRNA modifications maintains proteome integrity. *Cell* 161: 1606-1618, 2015.
37. Guo F, Cen S, Niu M, Javanbakht H and Kleiman L: Specific inhibition of the synthesis of human lysyl-tRNA synthetase results in decreases in tRNA(Lys) incorporation, tRNA(3)(Lys) annealing to viral RNA, and viral infectivity in human immunodeficiency virus type 1. *J Virol* 77: 9817-9822, 2003.
38. Chatzilakou E, Hu Y, Jiang N and Yetisen A: Biosensors for melanoma skin cancer diagnostics. *Biosens Bioelectron* 250: 116045, 2024.
39. Mao Y, Yan R, Li A, Zhang Y, Li J, Du H, Chen B, Wei W, Zhang Y, Summers C, *et al*: Lentiviral vectors mediate Long-term and high efficiency transgene expression in HEK 293T cells. *Int J Med Sci* 12: 407-415, 2015.
40. Stepanenko AA and Dmitrenko VV: HEK293 in cell biology and cancer research: phenotype, karyotype, tumorigenicity, and stress-induced genome-phenotype evolution. *Gene* 569: 182-190, 2015.
41. Ascierto PA, Kirkwood JM, Grob JJ, Simeone E, Grimaldi AM, Maio M, Palmieri G, Testori A, Marincola FM and Mozzillo N: The role of BRAF V600 mutation in melanoma. *J Transl Med* 10: 85, 2012.
42. Morris EJ, Jha S, Restaino CR, Dayananth P, Zhu H, Cooper A, Carr D, Deng Y, Jin W, Black S, *et al*: Discovery of a novel ERK inhibitor with activity in models of acquired resistance to BRAF and MEK inhibitors. *Cancer Discov* 3: 742-750, 2013.
43. Brożyna AA, Jóźwicki W, Carlson JA and Slominski AT: Melanogenesis affects overall and disease-free survival in patients with stage III and IV melanoma. *Hum Pathol* 44: 2071-2074, 2013.
44. Radomir MS, Tadeusz S, Przemysław MP, Chander R, Anna AB and Andrzej TS: Melanoma, melanin, and melanogenesis: The yin and yang relationship. *Front Oncol* 12: 842496, 2022.

45. Slominski A, Kim TK, Brożyna AA, Janjetovic Z, Brooks DL, Schwab LP, Skobowiat C, Jóźwicki W and Seagroves TN: The role of melanogenesis in regulation of melanoma behavior: Melanogenesis leads to stimulation of HIF-1 α expression and HIF-dependent attendant pathways. *Arch Biochem Biophys* 563: 79-93, 2014.
46. Radomir MS, Chander R, Jake YC and Andrzej TS: How cancer hijacks the body's homeostasis through the neuroendocrine system. *Trends Neurosci* 46: 263-275, 2023.
47. Vitiello M, Tuccoli A, D'Aurizio R, Sarti S, Giannecchini L, Lubrano S, Marranci A, Evangelista M, Peppicelli S, Ippolito C, *et al.*: Context-dependent miR-204 and miR-211 affect the biological properties of amelanotic and melanotic melanoma cells. *Oncotarget* 8: 25395-25417, 2017.
48. Militaru IV, Rus AA, Munteanu CVA, Manica G and Petrescu SM: New panel of biomarkers to discriminate between amelanotic and melanotic metastatic melanoma. *Front Oncol* 12: 1061832, 2023.
49. Kaczmarek-Szczepańska B, Kleszczyński K, Zasada L, Chmielniak D, Hollerung MB, Dembińska K, Pałubicka K, Steinbrink K, Swiontek Brzezinska M and Grabska-Zielińska S: Hyaluronic Acid/ellagic acid as materials for potential medical application. *Int J Mol Sci* 25: 5891, 2024.
50. Magina S, Vieira-Coelho MA, Serrão MP, Kosmus C, Moura E and Moura D: Ultraviolet B radiation differentially modifies catechol-O-methyltransferase activity in keratinocytes and melanoma cells. *Photodermatol Photoimmunol Photomed* 28: 137-141, 2012.



Copyright © 2025 Liu et al. This work is licensed under a Creative Commons Attribution-NonCommercial-NoDerivatives 4.0 International (CC BY-NC-ND 4.0) License.